A Novel Framework for Computing Unique People Count from Monocular Videos

Satarupa Mukherjee and Nilanjan Ray
Department of Computing Science, University of Alberta, Edmonton, Alberta T6G2E8, Canada

1 STAGE OF THE RESEARCH

I am a 5th year PhD student in the department of Computing Science in University of Alberta. I have passed my candidacy examination last year. I am currently in the final stage of my research and planning to defend by next semester.

In my PhD thesis, I have developed a novel people counting algorithm for computing unique people count from monocular videos. The algorithm has the capability of handling severe occlusion in addition to computing unique people count with exorbitant accuracy. Also it is online in nature, and does not accumulate error over time.

I have performed extensive experiments with the proposed algorithm on four standard datasets - the UCSD dataset (Chan et al., 2008), which consist of a full one hour video of $25,656$ frames, the FUDAN dataset (Tan et al., 2011) consisting of 1500 frames, the LHI dataset (Cong et al., 2009) which has 12 videos captured at different camera angles (90 degree, 65 degree and 40 degree) and of duration between 5 minutes and 15 minutes, and the PETS 2009 dataset (Krahnstoever et al., 2008) consisting of multiple camera views, targeted at the evaluation of various surveillance applications. The algorithm has produced more than 95% accuracy for most of these videos.

2 INTRODUCTION

People counting is important for solving many important applications like traffic management, detection of overcrowded situations in public buildings, tourist flow estimation, surveillance and many others. It is also a significant component in video analytics. By **unique people count**, we mean the computation of the total number of people in a specific time interval by counting a person only once while the person is present within a field of view (FOV) or a region of interest (ROI) within the FOV.

People counting systems can be roughly categorized into computer vision based and non-computer vision based techniques. The non-computer vision based systems use many different technologies (Box and Oppenlander, 2010), each with its own advantages and disadvantages. Probably the most straightforward system is the tally counter or clicker counter. It has a very simple working mechanism where pressing a button activates the count. However, the method needs human intervention, which is both labour and cost intensive. A very accurate people counting system is the mechanical counter, known as the turnstile, which needs to be turned by the individual each time he/she crosses it in order to take into account the individual count. However again, this method is invasive and disruptive. Laser beam-based sensors are among the non-invasive methods used frequently in railway stations. These methods are inexpensive, but they are not suitable for counting people in outdoor environments, because their performance can be negatively affected when subjected to direct sunlight. Another well-known non-invasive people counter is based on thermal sensors. However, once again, they are sensitive to ambient temperatures.

Computer vision-based solutions to date are mainly based on methods that use either a camera network or a monocular video. The network of multiple cameras is one of the most advanced technologies used for people counting. It takes into account different views of people with different camera angles to avoid occlusion. But setting up of the system can be costly and the process may often be cumbersome due to lack of resources. Moreover, homography constraints often need to be applied (Black and Ellis, 2006) for finding out correspondences among views of people obtained from multiple cameras in order to perform any kind of tracking or counting. The homography computation may also lead to the occurrence of transfer errors (summation of the projection error in each camera view for a pair of correspondence points) that needs to be dealt with. Our proposed approach to finding the unique people count is based on monocular videos. Our principal motivation is to make use of existing cameras and avoid expensive camera network setup and maintenance.

3 OUTLINE OF OBJECTIVES

Based on the above discussion, the objectives of my PhD thesis are as follows -

i. Compute unique people count over a certain interval of time from monocular videos.

ii. Make use of existing cameras by avoiding expensive camera setup and maintenance.

iii. Overcome occlusion problems and still obtain remarkable people count accuracies.

iv. Apply the algorithm on different scenarios and various kinds of human figures.

4 RESEARCH PROBLEM

My PhD thesis aims to develop a robust algorithm, the input of which is a monocular video consisting of human views and the output will be the total unique count of people within certain duration of the video.

The aim of the algorithm is its application towards real life problems. To avoid the expensive and also challenging video camera network system, it works on the view taken from a single camera. Finally, apart from dealing with sparse crowds, the algorithm is able to deal with large as well as dense crowds. Hence, it is capable of handling occlusions.

5 STATE OF THE ART

The computer vision based algorithms for people counting from monocular videos are mainly used for finding out two types of counts - frame based people count and unique people count. Frame based count is also known as density estimation.

The frame based people counting algorithms count people in individual video frames with reasonable accuracy even in the presence of occlusions (Chan et al., 2008; Chan and Vasconcelos, 2012; Chan and Vasconcelos, 2009; Conte et al., 2010; Tan et al., 2011; Lempitsky and Zisserman, 2010). These methods use extracted features from individual frames and count the number of people in each frame with the help of machine learning techniques that map the extracted features to the number of people present in the frame. But these methods fail to count the unique number of people present in a video over an interval of time, as they do not consider the correspondence of the same person over multiple frames. For example, if there are n people in the first frame and one person enters, while another person exits the FOV in the second frame, the frame based counting will produce n as the people count for the second frame. However, the unique count of people for the two frames should be $n+1$.

The computer vision based solutions to unique people count can be further categorized into three types: a) the detection and tracking based approach (Harasse et al., 2005; Kim et al., 2002; Zeng and Ma, 2010), b) the visual feature clustering based approach (Brostow and Cipolla, 2006; Rabaud and Belongie, 2006) and c) the line of interest (LOI) counting approach (Ma and A.B.Chan, 2013; Cong et al., 2009; Kim et al., 2008). The first two individual based analyses are somewhat successful for low density crowds or overhead camera views, but they are not competent enough for large crowds. In these types of views, there is too much occlusion, or people are depicted by only a few pixels or the situations are too challenging for tracking. The LOI counting methods are capable of handling occlusion, but these methods have received relatively less attention so far.

The detection and tracking based approaches (Harasse et al., 2005; Kim et al., 2002; Zeng and Ma, 2010) count people by detecting individuals in an image and creating corresponding trajectories by tracking them. The number of trajectories in an interval of time accounts for the number of people. This technique works well for situations where the object size is large, the crowd is not too dense and occlusion is not severe. Large object size helps in the detection as there are enough image pixels to depict the object. Tracking is failsafe for overhead FOVs where little or no occlusion is present. In case of whole body views, where partial occlusion is present, particle filter based tracking can be applied. Applying the detection-tracking approach becomes difficult in dense crowds where each person is depicted by only a few image pixels and people occlude each other in complex ways. Detection becomes challenging due to both occlusion and the small sizes of people. Occlusion also poses a difficult challenge for tracking.

The visual feature trajectory clustering methods (Brostow and Cipolla, 2006; Rabaud and Belongie, 2006) cluster feature trajectories that exhibit coherent motion and the number of clusters is used as the number of moving objects. This type of method requires sophisticated trajectory management, like handling broken feature tracks due to occlusions or measuring similarities between trajectories of different length. Thus, in crowded environments, it is frequently the case that coherently moving features do not belong to the same person. Thus, equating the number of people to the number of trajectory clusters becomes quite error prone. Once again, occlusion is a serious bottleneck for these methods too.

The LOI counting methods (Ma and A.B.Chan, 2013; Cong et al., 2009; Kim et al., 2008) have received much less attention so far. The basic principle here is to construct a temporal image at the LOI over a period of time. Next, the temporal image is converted to a cumulative count of people that crossed the LOI. But, often the methods are incapable of handling dense crowds and the methods may not perform well if the walking speed varies a lot within the crowd.

6 METHODOLOGY

The novel framework discussed in this paper, has a monocular video as its input, consisting of human views and the output of the framework is the total unique count of people within a certain duration of the video. The framework deals with both sparse as well as dense crowds, because it is capable of handling occlusions. Finally, a major advantage of the proposed framework is that it is online in nature and does not accumulate error over time.

We achieve the unique people count by a ROI analysis that is in a sense similar to the control volume analysis in fluidics describing the flow of fluid mass in/out/across a volume. Given a ROI within the FOV of a monocular video, our method counts the number of unique people who have entered or left the ROI within a short period of time. Thus, we are able to compute the influx and/or the outflux rate of unique people at any time instant. Summing these rates between any two time points provide us with the unique people count. Our method achieves this feat by combining frame-based people counting (a supervised machine learning method) with a simple ROI boundary tracker. Because, our method only computes pixel correspondence at the ROI boundary over a short period, it is able to cope well with occlusions. In this manner, our framework passes the responsibility of people count in the presence of occlusions to the supervised learner, and avoids object tracking altogether. The proposed method differs significantly from the LOI methods, as we do not rely on any temporal image generation and their analysis. Note also that LOI counting method relies on straight lines of interest, while our ROIs do not have such shape restrictions.

6.1 Background

Our proposed unique people count utilizes two techniques: a) frame based count and b) ROI boundary tracking. We discuss these two components in this section.

(a) Frame based Count. The general idea here is to extract features from an image frame and map these features to the number of people present in the image frame. This mapping is achieved by supervised machine learning methods, such as Gaussian Process regression (Chan et al., 2008).

The features that are taken into account include foreground features obtained from a background subtraction method and texture features. Based on empirical experiments, the background subtraction algorithms chosen for our framework are the Approximate Median method (McFarlane and Schofield, 1995) for the UCSD and the PETS 2009 datasets, Mixture of Gaussians method (Stauffer and Grimson, 1999) for the FUDAN dataset and ViBe (Barnich and Droogenbroeck, 2011) for the LHI dataset. The features considered for the frame based count are as follows:

i. Segment features are extracted to capture properties like shape, size etc. by computing a) foreground area, b) perimeter of foreground area, and c) perimeter-area ratio.

ii. Edge features, such as a) number of edge pixels, and b) edge orientation are computed. Edges within a segment are strong cues about the number of people in it.

iii. Texture features - Texture features, which are based on the gray-level cooccurrence matrix, are used for estimating the number of pedestrians in each segment (Chan et al., 2008; Tan et al., 2011). The image is first quantized into eight gray levels and masked by the segment. The joint probability of neighboring pixels i and j within the image frame I, $p(I(i),I(j) \mid \theta)$ is then estimated for four orientations $\theta \epsilon \{0^\circ, 45^\circ, 90^\circ, 135^\circ\}$.

  a Homogeneity: the texture smoothness, $g_\theta = \sum_{i,j} p(I(i),I(j) \mid \theta)/(1+|i-j|)$.

  b Energy: the total sum-squared energy, $e_\theta = \sum_{i,j} p(I(i),I(j) \mid \theta)^2$.

  c Entropy: the randomness of the texture distribution, $h_\theta = \sum_{i,j} p(I(i),I(j) \mid \theta) log p(I(i),I(j) \mid \theta)$.

Generally, features like foreground segmentation area or number of edge pixels should vary linearly with the number of people in each frame (Hou et al., 2010; Zhu, 2005). Foreground segmentation area versus the individual frame-based manual people count

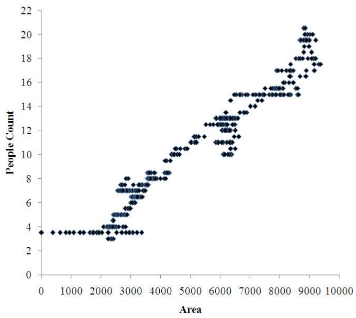

Figure 1: Plot of foreground segmentation area vs. people count on first 1000 frames of the UCSD dataset.

over the first 1000 frames of the UCSD dataset is plotted in Figure 1. It can be observed that the overall trend is almost linear with some local non-linearities. These local non-linearities occur due to different reasons like occlusion, segmentation errors in background subtraction, perspective foreshortening etc.

The non-linearities are modeled by including additional features, other than the segmentation areas, which are mentioned above and handled by a machine learner using a suitable kernel function. Here, we experiment with two machine learners which are capable of handling non-linear relationships- Gaussian Process (GP) Regressor (Rasmussen and Williams, 2006) and Support Vector Regressor (SVR) (Smola and Scholkopf, 1998).

We choose the UCSD dataset to evaluate the performance of the machine learners as it has many dense crowd instances. For training, the number of people is counted manually on 500 frames with variable crowd densities and the features of each frame within the ROIs are extracted. Next, the machine learners are trained with these extracted features and the corresponding people count in each frame within the ROI to learn the relationship between the two. The performance of the machine learners is then evaluated on 1000 validation frames that are different from the training frames. Manual count is also generated on these 1000 validation frames to perform the quantitative comparison between the two machine learners.

Figure 2 plots the predicted count versus the manual count for both the machine learners on the 1000-frame validation set. The dotted lines plot the predicted count from the machine learner, whereas the solid lines denote the true count produced manually. Both the GP Regressor and the SVR performs well on all of the validation set. A quantitative analysis based on mean squared error, mean absolute error and percentage of mean absolute error is reported in Table I. Here it can be seen that the performance of the GP Regressor is slightly better than that of the SVR. So,

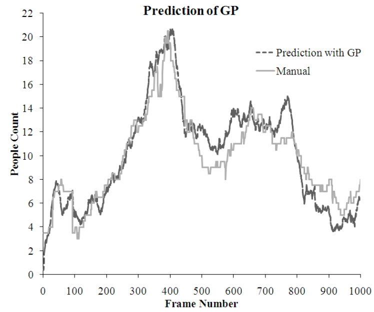

(a)

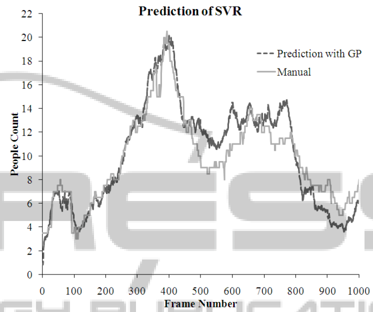

(b)

Figure 2: Performance evaluation of the two machine learners.

we chose GP for our framework.

The kernel of the GP or SVR is a combination of both linear and squared exponential kernels (RBF) (Chan et al., 2008):

$$k(x_p,x_q) = \alpha_1(x_p^T x_q + 1) + \alpha_2 e^{\frac{-\|x_p - x_q\|^2}{\alpha_3}} + \alpha_4\delta(p,q),$$

where x_p and x_q are the p-th and q-th feature vectors and $\alpha = \{\alpha_1, \alpha_2, \alpha_3, \alpha_4\}$ are the hyperparameters.

(b) Boundary Tracking with Optical Flow. As has been mentioned earlier, our proposed unique people count is inspired by the control volume analysis in fluidics. Thus, we need to account for people leaving or entering the ROI. To mitigate the effect of occlusion, we avoid the tracking of individual people in our framework. Instead, we track pixels on the ROI boundary over a short period of time. A number of methods can be applied for tracking the ROI boundary. However, we choose a simple off-the-shelf optical flow (Horn and Schunck, 1981) technique principally to make our framework more accessible. The optical flow computes pixel motion between two consecutive image frames, taking into account brightness constancy. Optical flow has a rich history; we found that a very basic technique (Horn and Schunck, 1981) suffices for boundary tracking in our application. We have used a publicly available implementation with

Table 1: Performance of GP and SVR on 1000 test frames.

Machine Learner	Mean Squared Error (No. of people squared/frame)	Mean Absolute Error (No. of people/frame)	Percent Mean Absolute Error (%)
GP	2.3818	1.2378	7.3
SVR	2.5151	1.3001	7.6

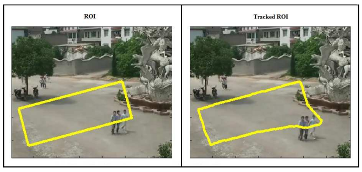

Figure 3: Actual ROI and Tracked ROI on an image of video 3-3 of the LHI dataset.

the default parameter settings in all our experiments. The original ROI and tracked ROI on an image of video 3-3 of the LHI dataset is plotted in Figure 3 to cite an example of boundary tracking.

6.2 Proposed Unique Count Framework

In this section, the proposed framework is presented. Our proposed framework counts the unique number of people who enter or leave an ROI within a time interval. In order to realize the framework, we assume availability of the following two functionalities discussed in the previous section:

Functionality 1. A ROI boundary tracker (*Track*) that is able to track the boundary of ROI R for a short while Δt.

Functionality 2. A machine learner (*Pred*), which is able to predict the number of people present within a ROI on a single video frame.

With these two functionalities, the following framework counts the number of unique people who have entered or left the ROI R.

Unique Influx and Outflux Count (UIOC) for $t = 0, 1, 2, 3, \ldots$.

$C^t \leftarrow Pred(I^t, R)$;
$R_d \leftarrow Track(I^t, I^{t+\Delta t}, R)$;
$\Delta C_{in} \leftarrow Pred(I^{t+\Delta t}, R \cup R_d) - C^t$;
$\Delta C_{out} \leftarrow C^t - Pred(I^{t+\Delta t}, R \cap R_d)$;
$F^t_{in} \leftarrow \Delta C_{in} / \Delta t$;
$F^t_{out} \leftarrow \Delta C_{out} / \Delta t$;
end
Output at time point t: F^t_{in}, F^t_{out}, C^t.

Unique influx count between t_1 and t_2 is $C^{t_1} + \sum_{t=t_1}^{t_2} F^t_{in}$, and unique outflux count between t_1 and t_2 is $C^{t_2} + \sum_{t=t_1}^{t_2} F^t_{out}$,

where,
I^t: Video frame at time t
R: Region of interest (ROI)
R_d: Deformed ROI due to boundary tracking between frames I^t and $I^{t+\Delta t}$.
ΔC_{in}: Unique influx between time points t and $t + \Delta t$
ΔC_{out}: Unique outflux between time points t and $t + \Delta t$
F^t_{in}: Influx rate of people at time t
F^t_{out}: Outflux rate of people at time t.

The *Track* functionality tracks the ROI boundary R from I^t through $I^{t+\Delta t}$. *Track* returns R_d, which is the deformed ROI due to the pixel motion at the boundaries of R. The *Pred* functionality counts the number of people within a ROI based on extracted image features. If a ROI neither consumes nor generates people, the influx and the outflux count over a period of time should be equal, assuming accurate performance by the two aforementioned functionalities. We refer to such a ROI as a (mass) *conserving* ROI. An example of a non-conserving ROI, where people get consumed and/or generated, is a view of an elevator, in which people enter or come out of.

Figure 4 explains why the framework works. The top left part of Figure 4, illustrates the positions of people and the ROI R at time instant t. The top right panel displays the positions of people at time instant $t + \Delta t$ as well as the deformed ROI R_d. Notice that R_d is a result of tracking the boundaries of R between t and $t + \Delta t$. The bottom left and right panels respectively show set union and intersection of the original ROI R and the deformed ROI R_d. For clarity, the positions of people at time instant $t + \Delta t$ at the bottom two panels are depicted by dots. Note that influx is given by $\Delta C^t_{in} = Pred(I^{t+\Delta t}, R \cup R_d) - Pred(I^t, R) = 4 - 3 = 1$, whereas outflux is given by $\Delta C^t_{out} = Pred(I^t, R) - Pred(I^{t+\Delta t}, R \cap R_d) = 3 - 1 = 2$. The total unique number of people produced by the influx count is $Pred(I^t, R) + \Delta C^t_{in} = 3 + 1 = 4$ and the total outflux count is $Pred(I^{t+\Delta t}, R) + \Delta C^t_{out} = 2 + 2 = 4$. As expected, these two numbers are equal, since the ROI here is a conserving one that neither consumes nor generates people.

The effect of occlusions is mitigated principally because of two reasons: (a) unlike object tracking, our boundary tracker, which computes pixel motion

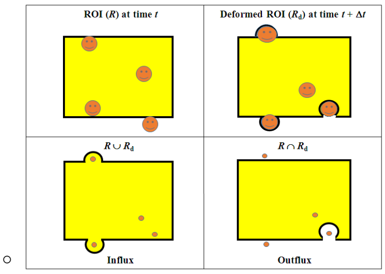

Figure 4: Explanation of influx and outflux.

on the ROI boundary for a short period, is hardly affected by occlusions, and (b) machine learner-based frame count is not much affected by occlusions either. Note that even if frame count is affected by occlusions to some extent at a particular time instant, chances are that in a later instant, the same occlusions will not exist in the scene. As a result, when we sum up the influx/outflux rates, the effect of occlusions is suppressed. Basically, by avoiding object tracking and/or track generations for an extended period, we bypass occlusions and pass the responsibility of tackling occlusions to the machine leaner. Our experiments validate this observation.

7 RESULTS AND DISCUSSIONS

For the UCSD dataset, we have chosen a rectangular ROI R, as shown in the top left panel of Figure 5. For the FUDAN dataset, our chosen ROI is shown in the top left panel of Figure 6. The top right panels in Figures 5 and 6 show the deformed ROI R_d. We have chosen to compute influx count for the UCSD dataset and outflux count for the FUDAN dataset. The bottom left panels in Figures 5 and 6 show respectively $R \cup R_d$ and $R \cap R_d$. The bottom right panels in Figures 5 and 6 show the foreground/background segmentations. It is noted that both the datasets have severe occlusions. Another challenge in the FUDAN dataset is that it also contains shadows of people.

We compute the influx count on the LHI dataset. For the LHI dataset, the ROIs are chosen as shown in Figure 7. Here, the ROI selection is decided based on the detection region considered in (Cong et al., 2009). The formula used for calculating accuracy is 100(1-(| Manual Count - Predicted Count |/Manual Count)) (Cong et al., 2009).

The timestep Δt is the only tunable parameter in our framework. On one hand, a large Δt would smooth out noisy predictions by the machine learner. On the other hand, a large Δt would make the boundary tracking more challenging due to occlusions. The timestep used for the application of the tracking routine varies for different datasets. These values are chosen based on our experiments with three different values on the first 100 frames. The experiments for the FUDAN dataset are shown in Table II.

UIOC performs well on all the datasets. The results for the UCSD and the FUDAN dataset including the accuracies are tabulated in Table III and IV respectively. UIOC also performs well on all 12 videos of the LHI dataset. The accuracies remain close to 95% for most datasets. Also, note that all types of camera angles and video lengths do not seems to decrease the accuracy as much as observed in Table V.

We demonstrate with experiments that our framework is competent enough to handle occlusions. We

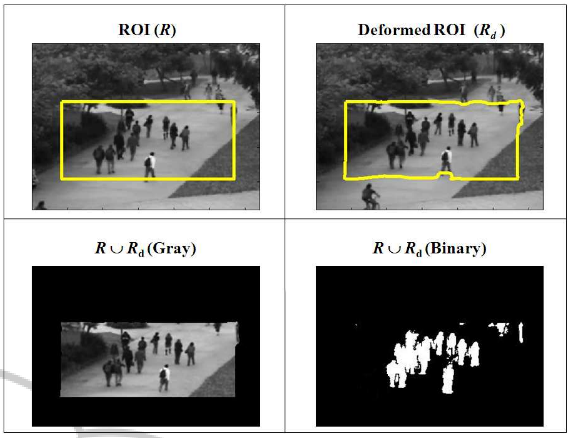

Figure 5: Visual Results on the UCSD dataset.

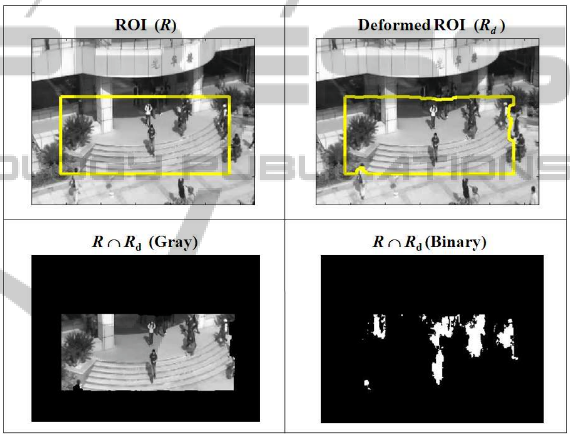

Figure 6: Visual Results on the FUDAN dataset.

Table 2: Accuracy for three different timesteps for the FUDAN dataset.

Δt (No. of Frames)	Accuracy (%)
20	91.35
25	98.46
30	93.22

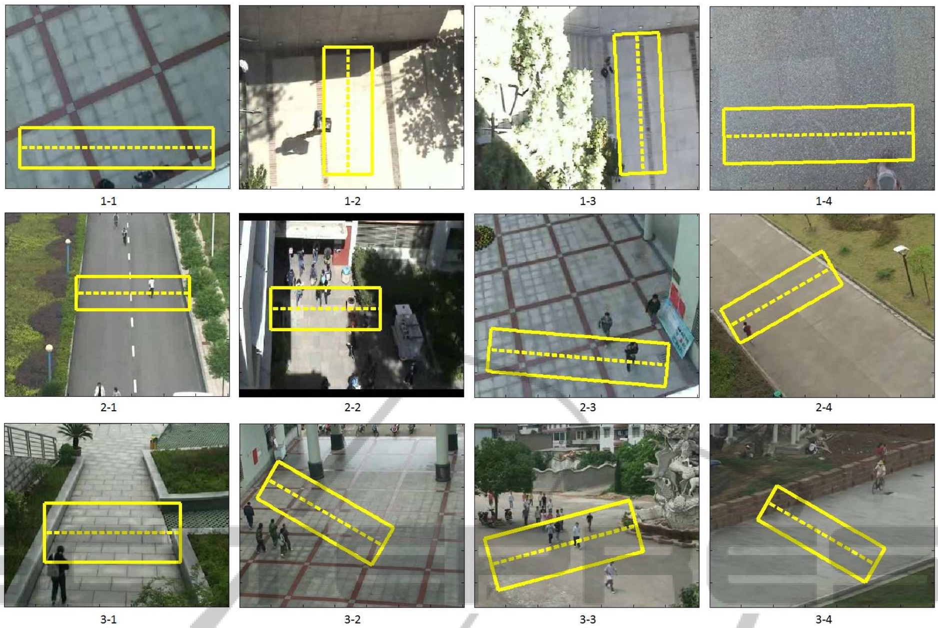

Figure 7: Different videos of the LHI dataset. The dotted lines are the LOIs of (Cong et al., 2009). The rectangles are our ROIs.

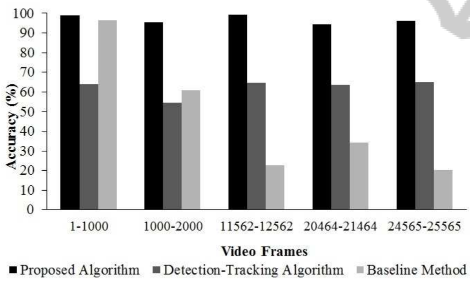

Figure 8: Performance evaluation of three algorithms.

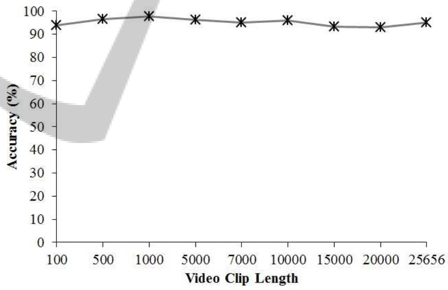

Figure 9: Accuracy of the proposed framework with increase of video clip lengths.

choose 5 mostly occluded video clips each of length 1000 from the UCSD dataset. We produce the experimental count from our framework on these 5 video clips along with the manual unique count to obtain the accuracy in Figure 8. In all the cases, the accuracy is more than 90% that shows that the framework performs well on occluded crowds.

We also want to illustrate experimentally that there is no error accumulation with the increase in length of video clips. Toward this end, unique people count is done on different length of video clips from the UCSD dataset and a plot of accuracy versus video clip lengths is shown in Figure 9. It is observed from the graph that the accuracy remains more or less flat when the number of frames is increased.

UIOC works as fast as 10 frames per second on a system with Intel(R), core(TM), DuO CPU, E8400 @ 3GHz. The system is implemented in openCV using the MATLAB implementation of the GP.

Performance of UIOC is compared with the method proposed by Zeng *et al.* (Zeng and Ma, 2010), which is a detection-tracking method for people counting and also with the Flow-Mosaicking method (Cong et al., 2009), which is a LOI counting method. UIOC is also compared with a baseline method. These comparisons are described next.

7.1 Comparison with a Baseline Method

The baseline method we devise here is as follows. Suppose, we know the average number of frames n_t for which a person is inside the ROI R on frame t. Then, a baseline estimate of the unique people count can be computed between two time points t_1 and t_2 as: $\sum_{t=t_1}^{t_2} Pred(I^t,R)/n_t$, where, as before, $Pred(I^t,R)$ predicts the number of people on frame I^t within the

ROI R. A few comments are in order here. First, not all the people are staying within the ROI for the same number of frames due to varying walking paces, and different entry and exit points. So, the above formula would indeed provide a crude estimate of the unique people count. Second, even estimating the average number of frames n_t is a nontrivial task. Instead of object tracking, we can try to find out the foreground pixel motion trajectories laid across the ROI. These trajectories would provide us with the average number of frames for which a foreground pixel stayed within the ROI. However, finding these trajectories is a nontrivial task, mainly because of occlusions. A practical and quick approximation to n_t can be obtained by dividing the distance d between a typical entry and exit point on the ROI border by the average foreground pixel speed s_t (obtained by optical flow) computed on frame t. With these approximations, the baseline method count turns into the formula: $(\sum_{t=t_1}^{t_2} s_t Pred(I^t, R))/d$.

Furthermore, we treat the distance d as a tunable parameter here. So, we choose its value by matching the baseline count with the manual count on a training set of the first 500 frames. We apply the baseline method on both the UCSD and FUDAN datset. The total unique count produced by the method for the datasets are 1324.19 and 121.77 respectively, while the manual counts are 1062 and 74. The comparison of accuracies of the proposed framework and the baseline method as demonstrated in Table III and Table IV shows that the proposed UIOC outperforms the baseline method for both the datasets.

The unique people count is also recorded for the baseline method on the same 5 mostly occluded video clips from the UCSD dataset of length 1000 used for UIOC. The result is plotted in Figure 8. Notice that on the first 1000 frames, the baseline method performed well, because we have tuned d on the first 500 frames. The comparison here clearly shows that UIOC outperforms much more in terms of accuracy, even in the occluded regions.

7.2 Comparison with a Detection-tracking Method

In Zeng *et al.*'s work, each individual person is detected in a frame and then tracked in consecutive frames until the person leaves the field of view (Zeng and Ma, 2010). The trajectory generated due to tracking represents a single individual. The number of trajectories denote the number of people during a time interval.

The detection here is a supervised method in which Zeng *et al.* use both Histogram of Gradients (HOG) (Dalal and Triggs, 2005) and Local Binary Pattern (LBP) (Ojala et al., 2002) features to detect the head and shoulders of people to avoid partial occlusion. For tracking, they use a particle filter tracker (Chateau et al., 2006).

Table 3: Accuracy of three algorithms on the UCSD dataset.

Algorithm	Predicted People Count	Manual People Count	Accuracy (%)
UIOC	1118.27	1062	94.70
Zeng *et al.*	727	1062	68.46
Baseline	1324.19	1062	75.31

Table 4: Accuracy of three algorithms on the FUDAN dataset.

Algorithm	Predicted People Count	Manual People Count	Accuracy (%)
UIOC	75.14	74	98.46
Zeng *et al.*	21	74	28.38
Baseline	121.77	74	35.45

Zeng *et al.*'s method is also applied on both the UCSD dataset and the FUDAN dataset. As it is a supervised method, 50% of the total number of frames is used for training and the remaining 50% for testing. Though the detection process is tried to be made robust by taking into account both HOG and LBP features, the detection performance was observed to be somewhat poor on the datasets used here. This happens mainly because of two reasons. Since the size of human beings is very small in the UCSD dataset, the detection process becomes complicated as there are fewer pixels on a human body to detect it properly. The second issue is the occlusion that plagues both detection and tracking.

The performance evaluations of the detection-tracking algorithm are tabulated in Table III for the UCSD dataset and Table IV for the FUDAN dataset showing that UIOC outperforms the detection-tracking algorithm for both the datasets.

Unique people count is also recorded for Zeng *et al.*'s method on the same 5 mostly occluded video clips from the UCSD dataset of length 1000 used for UIOC. The results are plotted in Figure 8. The comparison here clearly shows that UIOC outperforms much more in terms of accuracy, even in the occluded regions.

7.3 Comparison with a LOI Counting Method

The LOI counting method described in the Flow-Mosaicking method (Cong et al., 2009) counts the number of people crossing a specific line of interest based on flow velocity estimation and temporal image generation. This method was applied on 12 videos of the LHI dataset (Cong et al., 2009). The videos are captured with camera angles of 90, 65 and 40 degrees respectively. There are 4 videos corresponding to each angle and the videos have different views and different lengths. We have chosen ROIs similar to those used in the paper (Cong et al., 2009). These ROIs are shown in Figure 7. We run our UIOC framework on all 12 videos of the LHI dataset and provide a comparative study of our accuracies versus the accuracies of the Flow-Mosaicking method in Table V. We observe that the accuracy of our method on all 12 videos exceed those of the LOI counting method. We attribute the failure of the LOI method here on inaccuracies arise due to the analysis of the temporal images. In contrast, our method does not rely on any temporal images or their analysis.

7.4 Work on Multiple ROIs

In order to increase the accuracy of the UIOC framework, we apply it on multiple ROIs, rather than on a single ROI as shown in Figure 11. Apart from the ROI in the middle on which we train our machine learner, we take more ROIs to take different sample regions from the image. To avoid the increase of computational cost due to multiple ROIs, we plan to apply the machine learner only once. In order to incorporate this idea, initially we calculate the ratio of the number of people present in a ROI versus foreground area, denoted by α. The plot of α for the first 300 frames of the UCSD dataset is shown in Figure 10. The number of people used for obtaining this ratio is calculated on the training ROI, ie the ROI on which the machine learner is trained. By observing the graph in Figure 10, we note that α does not vary dramatically within a short period of time. Thus, we can calculate the influx count for ROIs with the following equation:

$$\Delta C_{in}^{t} = \alpha^{t+\Delta t} A^{t+\Delta t}(R \cup R_d) - \alpha^{t} A^{t}(R)$$

where,
$\alpha^t = Pred(I^t, R)/A^t(R)$
$\alpha^{t+\Delta t} = Pred(I^{t+\Delta t}, R)/A^{t+\Delta t}(R)$
$A^t(R)$: foreground area of ROI R at time t
R: actual ROI
R^d: deformed ROI due to boundary tracking
ΔC_{in}^{t}: influx at time t.

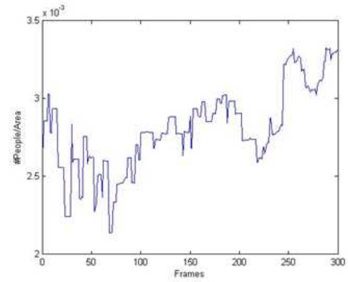

Figure 10: Plot of α over time.

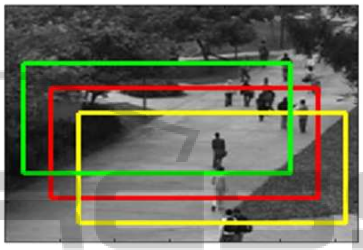

Figure 11: Multiple ROIs.

Once we get the total influx count for all the individual ROIs, we take the average to compute the final unique count. Number of ROIs is a design parameter here. On the training set, we empirically found that we obtained maximum accuracy with 3 ROIs. The experimental unique count achieved is 1078.41, whereas the manual count was 1062. The accuracy is 98.45% on the entire UCSD dataset. In comparison, the unique count was 94.70% with a single ROI previously.

8 ADDITION OF DIRECTIONALITY

In addition to total people count, we also intend to incorporate directionality in our framework. We test this idea on the UCSD dataset. In the UCSD dataset, the people flow goes mainly in two directions: north and south. In order to count the number of people heading north, we need to take into account the people exiting through the upper boundary i.e., the directional outflux through the upper boundary, because the people who are entering the ROI through the lower boundary are exiting the ROI through the upper boundary. Similarly, for counting the people heading south, we need to consider the people exiting through the lower boundary ie the directional outflux through the lower boundary.

Figure 12 explains how the directional counting works. The top left panel of Figure 12 illustrates the positions of people and the ROI R at time instant t.

Table 5: Comparative study of the UIOC method and the Flow-Mosaicking method (Cong et al., 2009) on the LHI dataset.

Camera Angle	Video name	Video Length (min:sec)	Total no. of pedestrians	Accuracy (%) UIOC method	Accuracy (%) Flow mosaicking method
90	1-1	8:59	256	99.64	97.66
	1-2	14:48	247	97.02	94.33
	1-3	4:30	23	96.61	95.65
	1-4	5:30	180	98.63	93.33
65	2-1	11:29	62	98.27	83.87
	2-2	8:24	300	96.21	84.67
	2-3	3:45	42	91.26	90.48
	2-4	4:40	44	99.72	86.36
40	3-1	7:16	29	97.25	82.76
	3-2	25:35	267	94.64	93.26
	3-3	13:08	288	99.26	93.75
	3-4	10:08	40	93.08	87.50

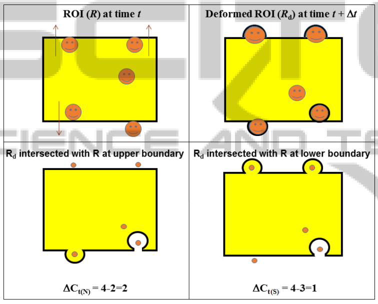

Figure 12: Addition of directionality.

The top right panel displays the positions of people at time instant $t + \Delta t$ as well as the deformed ROI R_d. R_d is a result of tracking the boundaries of R between t and $t + \Delta t$. The bottom left panel shows R_d intersected with R at the upper boundary, which we need in order to compute the number of people heading north. The bottom right panel shows R_d intersected with R at the lower boundary which we need in order to compute the number of people heading south. The number of people heading north is given by the difference of the number of people present in the actual ROI and the number of people present in the deformed ROI, which is formed from the intersection of R and R_d at the top i.e., $\Delta C_N^t = 4 - 2 = 2$. On the other hand, the number of people heading south is given by the difference of the number of people present in the actual ROI and the number of people present in the deformed ROI, which is formed by the intersection of R and R_d at the bottom i.e., $\Delta C_S^t = 3 - 2 = 1$. Summing ΔC_N^t and ΔC_S^t and dividing a specific time interval, we get the total number people moving north and the total number of people moving south respectively.

We test the method on the first video of the UCSD dataset, which has the densest crowd. We manually count the number of people heading north and south separately and then run our framework to get the experimental count. We achieve more than 90% accuracy in both cases as tabulated in Table VI.

Table 6: Performance of UIOC for directionality.

Direction	Manual People Count	Accuracy (%)
North	183	94.17
South	204	93.23

9 APPLICATION ON MULTIPLE VIEWS

For extending our framework towards more benchmark datasets, we apply it on multiple views of the PETS 2009 dataset. (S1-L2 view, Time 14-31).

In order to apply the UIOC framework on multiple views, the first step is to merge multiple views together in order to choose a ROI. Using a simple program that uses the OpenCV library, the views are merged by their overlapping areas to create an extended view. This is accomplished by manually choosing corresponding points between the source images (views two, three and four) and the destination image (view one) which are the four views presented in Figure 13. Using these points and OpenCV library functions, the homography among the views is found and used to transform views two, three, and four into the closest match of view one.

Once the three views are transformed, all four views are superimposed on top of one another for the actual merging. Figure 14 shows the merged view. The ROI is then chosen on the merged image. For each view that is transformed, the coordinates of the chosen ROI are transformed using the inverse of the transformation matrix that is used to transform the image to match view one. In this way, the newly transformed ROI corresponds roughly to the correct location on each original view. Also, any points too close to the edges or out of bounds have to be moved in. In the case of the PETS data, as all the views have significant overlap and there is not much room to lose people in, the count for each view should theoretically be almost the same. Therefore, at the end of the program, the average count among all four views is taken as the final estimated people count. The actual count for the selected ROI is 38, and the estimated count is 38.49 which produces 98.71% accuracy.

We compare our results with an existing multi-camera person tracking work (Krahnstoever et al., 2008). According to (Krahnstoever et al., 2008), the people count accuracy on PETS 2009 S1-L2 dataset (Time 14-31) is almost 82% whereas our accuracy is 98.71% which we achieve without taking into consideration any homography constraints.

So, the UIOC framework, though initially developed for monocular videos, is proved to be flexible enough to perform well even on a network of cameras capturing multiple human views.

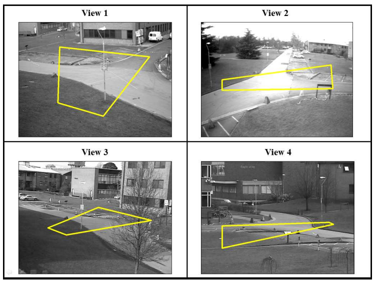

Figure 13: The four different views and the chosen ROIs on the PETS 2009 S1-L2 dataset.

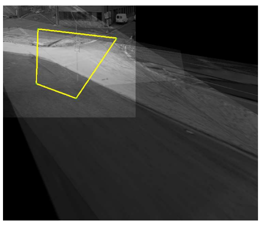

Figure 14: Merged view of PETS dataset.

10 CONCLUSIONS

We design a novel framework for finding the unique people count on monocular videos. Our framework is capable of counting the total number of people in a specific time interval by overcoming occlusion, which is one of the most dominant problems in the domain of computer vision based solutions to people counting. We achieve more than 95% accuracy on numerous publicly available benchmark videos. Our method outperforms two state of art algorithms and a baseline method. We even extend our framework to work on multiple views with highly satisfactory accuracy.

11 EXPECTED OUTCOME

The expected outcome of my research is to produce a people counting software, the input of which will be a monocular video and the output will be the total unique count of people within the video. We expect to produce more than 90% accuracy in all kinds of human video. The software is user friendly and can generate results in real time. Thus it is viable for commercialization. Once commercialized, the software can be used in many real life scenarios like traffic management, surveillance videos and many other video analytic applications as discussed earlier in this paper.

ACKNOWLEDGEMENTS

The authors would like to thank Dr. Yang Cong for the LHI dataset. The authors also acknowledge the following sources of funding for this work: NSERC, AQL Management Consulting Inc., and Computing Science, University of Alberta.

REFERENCES

Barnich, O. and Droogenbroeck, M. V. (2011). Vibe: A universal background subtraction algorithmfor video sequences. *Transactions in Image Processing*, 20:1709–1724.

Black, J. and Ellis, T. (2006). Multi camera image tracking. *Image and Vision Computing*, 24:1256–1267.

Box, P. C. and Oppenlander, J. C. (2010). Manual of traffic engineering studies. Technical report, Institute of Transportation Engineers.

Brostow, G. J. and Cipolla, R. (2006). Unsupervised bayesian detection of independent motion in crowds. In *CVPR*, pages 594–601.

Chan, A. B., Liang, Z. S. J., and Vasconcelos, N. (2008). Privacy preserving crowd montioring: counting people without people models or tracking. In *CVPR*, pages 1–7.

Chan, A. B. and Vasconcelos, N. (2009). Bayesian poisson regression for crowd counting. In *ICCV*, pages 1–7.

Chan, A. B. and Vasconcelos, N. (2012). Counting people with low-level features and bayesian regression. In *TIP*, volume 21, pages 2160–2177.

Chateau, T., GayBelille, V., Chausse, F., and Lapreste, J. (2006). Real-time tracking with classifiers. In *ECCV*, pages 218–231.

Cong, Y., Gong, H., Zhu, S., and Tang, Y. (2009). Flow mosaicking: Real-time pedestrian counting without scene-specific learning. In *CVPR*, volume 1093-1100.

Conte, D., Foggia, P., Percannella, G., Tufano, F., and Vento, M. (2010). Counting moving people in videos by salient points detection. In *ICPR*, pages 1743–1746.

Dalal, N. and Triggs, B. (2005). Histograms of oriented gradients for human detection. In *CVPR*, pages 886–893.

Harasse, S., Bonnaud, L., and Desvignes, M. (2005). People counting in transport vehicles. *Transactions on Engineering, Computing and Technology*, 4:221–224.

Horn, B. and Schunck, B. (1981). Determining optical flow. *Artificial Intelligence*, 17:185–203.

Hou, C. P., Zhang, C. S., Wu, Y., and Nie, F. P. (2010). Multiple view semi-supervised dimensionality reduction. *Pattern Recognition*, 43:720–730.

Kim, J., Choi, K., Choi, B., and Ko, S. (2002). Real-time vision-based people counting system for the security door. *ITC-CSCC*, pages 1418–1421.

Kim, Y. S., Lee, G. G., Yoon, J. Y., Kim, J. J., and Kim, W. Y. (2008). A method of counting pedestrians in crowded scenes. In *International Conf. on Intelligent Computing*, pages 1117–1126.

Krahnstoever, N., Yu, T., Patwardhan, K. A., and Gao, D. (2008). Multi-camera person tracking in crowded environments. In *PETS workshop*, pages 1–7.

Lempitsky, V. and Zisserman, A. (2010). Learning to count objects in images. *NIPS*.

Ma, Z. and A.B.Chan (2013). Crossing the line: Crowd counting by integer programming with local features. In *CVPR*, pages 2539–2576.

McFarlane, N. J. B. and Schofield, C. P. (1995). Segmentation and tracking of piglets in images. *Machine Vision and Applications*, 8:187–193.

Ojala, T., Pietikainen, M., and Maenpaa, T. (2002). Multiresolution gray scale and rotation invariant texture analysis with local binary patterns. In *PAMI*, volume 24, pages 971–987.

Rabaud, V. and Belongie, S. J. (2006). Counting crowded moving objects. In *CVPR*, pages 705–711.

Rasmussen, C. E. and Williams, C. K. I. (2006). *Gaussian Processes for Machine Learning*. MIT Press, Cambridge, MA.

Smola, A. and Scholkopf, B. (1998). A tutorial on support vector regression. NeuroCOLT Technical Report NC-TR-98-030, Royal Holloway College, University of London, UK.

Stauffer, C. and Grimson, W. (1999). Adaptive background mixture models for real-time tracking. In *CVPR*, pages 246–252.

Tan, B., Zhang, J., and Wang, L. (2011). Semi-supervised elastic net for pedestrian counting. *Pattern Recognition*, 44:2297–2304.

Zeng, C. and Ma, H. (2010). Robust head-shoulder detection by pca-based multilevel hog-lbp detector for people counting. In *ICPR*, pages 2069–2072.

Zhu, X. J. (2005). Semi-supervised learning literature survey. Technical Report Technical Report 1530, University of Wisconsin-Madison.